Talanta Open 11 (2025) 100412

Contents lists available at ScienceDirect

Talanta Open

journal homepage: www.sciencedirect.com/journal/talanta-open

Strong toxic gas detection on penta-BCP monolayers: Insights from DFT calculations

Thanasee Thanasarnsurapong [a], Suchanuch Sringamprom [a], Pakpoom Reunchan [a], Weekit Sirisaksoontorn [b], Sirichok Jungthawan [c], Piyanooch Nedkun [d], Jariyanee Prasongkit [e,*], Adisak Boonchun [a,*]

[a] Department of Physics, Faculty of Science, Kasetsart University, Chatuchak, Bangkok 10900, Thailand
[b] Department of Chemistry, Faculty of Science, Kasetsart University, Chatuchak, Bangkok 10900, Thailand
[c] Center of Excellence in Advanced Functional Materials, Suranaree University of Technology, Nakhon Ratchasima 30000, Thailand
[d] Department of General Science, Kasetsart University Chalermphrakiat Sakon Nakhon Province Campus, Sakon Nakhon, 47000, Thailand
[e] Division of Physics, Faculty of Science, Nakhon Phanom University, Nakhon Phanom 48000, Thailand

ARTICLE INFO

Keywords:
Gas sensor
DFT
2D materials

ABSTRACT

Rapid and accurate detection of toxic gases remains important for industrial safety and environmental well-being. This study examines the potential of penta-BCP monolayer as a high-performance toxic gas sensor utilizing the robust framework of density functional theory (DFT). Penta-BCP exhibits strong and selective interactions with specific toxic gas molecules, including CO, NO, and NO_2. This results in the remarkable ability to readily capture these harmful gases while demonstrating minimal interaction with non-toxic counterparts such as H_2, N_2, CO_2, and CH_4, underlining its exceptional selectivity. Furthermore, penta-BCP has a significantly shorter recovery time for NO and NO_2 gases compared to penta-BCN, which has a similar structure. These findings collectively position penta-BCP as a frontrunner for the next generation of toxic gas sensors, paving the way for enhanced environmental monitoring and improved public health protection.

1. Introduction

The rapid growth of industries in the past century has led to serious health problems due to the release of harmful gases, including carbon monoxide (CO), nitrogen oxide (NO), and nitrogen dioxide (NO_2). This has driven the development of reliable sensors capable of detecting these dangerous gases. Recently, two-dimensional (2D) materials have emerged as promising candidates for this purpose due to their unique advantages, such as large surface area and numerous active sites for interacting with gas molecules, as demonstrated in several studies [1–5]. Furthermore, materials such as graphene and its derivatives have shown remarkable potential in gas-sensing applications owing to their high sensitivity and stability [6–8].

Creating highly sensitive and selective gas sensors requires materials capable of strongly reacting with target gas molecules and quickly recovering to their original state. Among various 2D materials, pentagonal structures have garnered attention due to their enhanced interaction with harmful gases [9,10]. For instance, biphenylene-based sensors exhibit remarkable anisotropy and selectivity for detecting gases such as NO_2, NH_3, and SO_2, outperforming traditional graphene-based systems in terms of sensitivity and response time [7,11]. Similarly, Janus ZrBrCl monolayers have demonstrated tunable sensitivity to NO and NO_2 through strain engineering [12].

Besides the common 2D hexagonal based structures, numerous 2D materials with pentagonal based structures have been proposed [9, 13–21]. Due to their unique configurations, pentagonal materials exhibit fascinating electronic properties and hold promise for a wide range of applications, including Li-ion battery technology [22–24] and gas sensing [25,26]. For instance, building upon recent advancements in gas-sensing technologies, Sringamprom et al. theoretically demonstrated that binary penta-$BeAs_2$ monolayers exhibit exceptional toxic gas-sensing performance for NO, NO_2, and CO, highlighting their high sensitivity and rapid recovery times [26].

In this study, first-principles calculations are employed to explore the gas-sensing potential of the ternary penta-BCP. Analysis of adsorption energies, charge transfers, and electronic structures reveals preferential

* Corresponding authors.
E-mail addresses: jariyanee.prasongkit@npu.ac.th (J. Prasongkit), adisak.bo@ku.th (A. Boonchun).

https://doi.org/10.1016/j.talo.2025.100412
Received 2 January 2025; Received in revised form 17 January 2025; Accepted 17 January 2025
Available online 21 January 2025

adsorption of this material towards toxic gases such as CO, NO, and NO_2, with negligible interaction with non-toxic gases (H_2, N_2, CO_2, and CH_4). This aligns with findings from Luo et al., who reported selective detection capabilities in vdW heterojunctions [11].

The exclusion of oxygen (O_2) molecules in this study is deliberate, as their interaction with 2D penta-materials remains a topic of debate. While some researchers argue that O_2 reacts readily with these materials [27–30], potentially hindering selectivity, others, such as Jiang, suggest weaker physisorption behavior [25]. Our findings reaffirm the penta-BCP monolayer's potential as a selective toxic gas sensor, similar to other high-performance materials such as Sc-decorated biphenylene for hydrogen sensing [6,7].

2. Computational methods

Our theoretical calculations were based on the density functional theory (DFT) built into the Vienna *Ab-initio* Simulation Package (VASP) [31,32]. The plane-wave basis set is augmented with projector-augmented waves (PAW) as described by Blöchl [33]. A kinetic energy cutoff of 520 eV is employed for the plane-wave expansion. The geometry optimization utilizes the Perdew-Burke-Ernzerhof (PBE) functional [34] and is carried out until the total Hellmann-Feynman forces are below 0.01 eV/Å, with an energy convergence criterion of 10^{-5} eV. A k-point grid of $2 \times 2 \times 1$ is used to integrate over the first Brillouin zone within the Γ-centered Monkhorst-Pack scheme [35]. To accurately capture the interactions within layered materials, the long-range van der Waals (vdW) forces are incorporated using the DFT-D3 functional proposed by Grimme [36]. In order to reduce the self-interactions between the monolayer and its periodic image, a vacuum layer of 20 Å is included along the direction perpendicular to the crystal plane.

3. Results and discussion

The penta-BCP monolayer is constructed by replacing the nitrogen (N) atoms in the penta-BCN structure [14] with phosphorus (P) atoms. Fig. 1(a) shows the optimized atomic arrangement of the penta-BCP monolayer, where blue spheres represent boron (B) atoms, silver spheres represent phosphorus (P) atoms, and gray spheres represent carbon (C) atoms. Penta-BCP and penta-BCN share the same crystal structure, which belongs to the $P2_1$ symmetry (space group 4). Our calculations reveal optimized lattice parameters of $a = 3.68$ Å and $b = 4.11$ Å, which agree with previously reported values ($a = 3.67$ Å and $b = 4.12$ Å) [19]. Fig. 1(b) shows the electronic band structure of the penta-BCP monolayer, confirming its semiconducting nature. This work calculated a bandgap of 1.97 eV at the PBE level, consistent with the previously reported value of 1.97 eV [19].

To assess the strength of the interaction between various gas molecules and the penta-BCP monolayer, we calculated the adsorption energy (E_{ad}) using the following equation:

$$E_{ad} = E_{\mathrm{BCP+gas}} - E_{\mathrm{BCP}} - E_{gas}, \quad (1)$$

where $E_{\mathrm{BCP+gas}}$ represents the total energy of a single gas molecule adsorbed on a perfect 2×2 supercell of the penta-BCP monolayer system, E_{BCP} is the energy of the clean 2×2 supercell, and E_{gas} is the energy of an isolated gas molecule.

Various potential adsorption sites were considered to identify the most stable configurations for gas adsorption on the penta-BCP monolayer, as shown in Fig. 1(a). These sites include the top positions (T1-T3), bridge positions (B1–B3), and the center of the hollow pentagon (H1 and H2). For each position, the center of mass of the gas molecule was precisely placed. Additionally, three different orientations were examined for each adsorbed gas. For example, NO was considered both parallel and perpendicular to the monolayer, with the oxygen atom positioned above or below the nitrogen atom. Fig. 2 presents the most

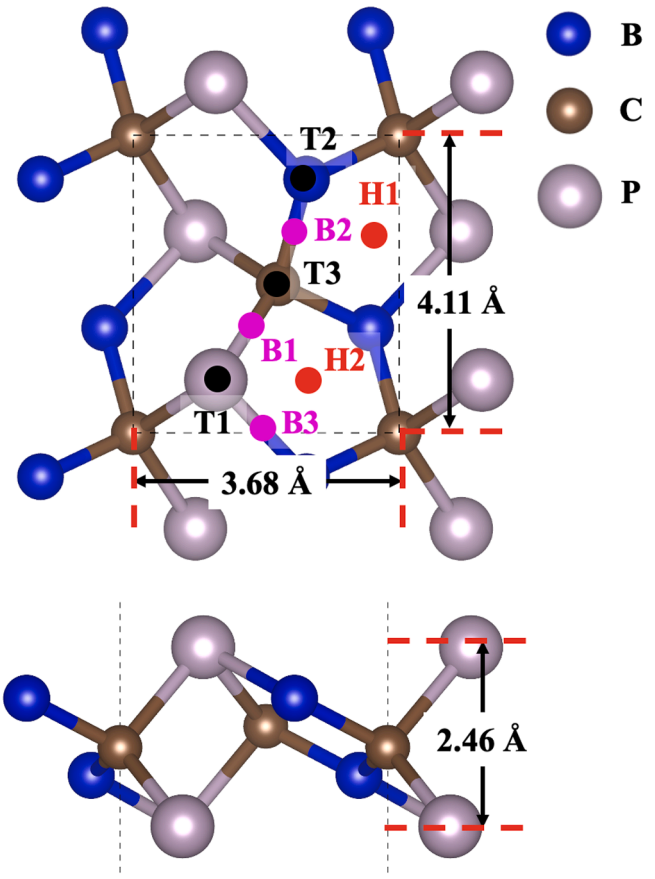

Fig. 1. Unit cell of pentagonal BCP.

stable configurations for several gas molecules in the penta-BCP structure[14], including H_2, N_2, CO, CO_2, CH_4, NO and NO_2.

As shown in Table 1, the calculated adsorption energies for various gases adsorbed on the penta-BCP monolayer show a distinction between toxic and non-toxic gas molecules. The adsorption energies for H_2, N_2, CO_2 and CH_4 are significantly weaker, ranging from −0.079 eV to −0.198 eV, compared to the much stronger adsorption energies of CO, NO and NO_2 (− 0.988, − 1.010, and −1.496 eV, respectively). This indicates a strong preference for toxic gas adsorption on the penta-BCP monolayer.

The adsorption behavior of CO_2 and NO_2 differs from CO and NO. While CO and NO bond directly with the substrate through C–B and N–B bonds, respectively, CO_2 and NO_2 molecules are adsorbed parallel to the penta-BCN layer. Additionally, the adsorption distances (d) for the toxic gas molecules (CO, NO and NO_2) on penta-BCP are significantly shorter (1.46–1.56 Å), close to typical bond lengths in solid materials, suggesting chemisorption. In contrast, non-toxic gas molecules exhibit weak van der Waals interactions (physisroption) with the penta-BCP monolayer, as evidenced by the larger adsorption distances that range from 3.07 to 3.22 Å.

Compared to other pentagonal materials, penta-BeP_2 exhibits moderate adsorption energies for toxic gas molecules like CO, NO, and NO_2 (ranging from −0.70 to −0.90 eV) as reported previously.[25] In contrast, penta-BCP demonstrates a stronger interaction, with adsorption energies for these same gas molecules ranging between −0.99 and −1.50 eV. This signifies a significantly stronger binding between toxic gases and penta-BCP compared to penta-BeP_2.

Furthermore, both penta-BCP and penta-BeP_2 exhibit negligible interaction with common non-toxic gases such as H_2, N_2, and CO_2, which have adsorption energies less than −0.20 eV, highlighting their potential for selective adsorption of toxic gases without significant

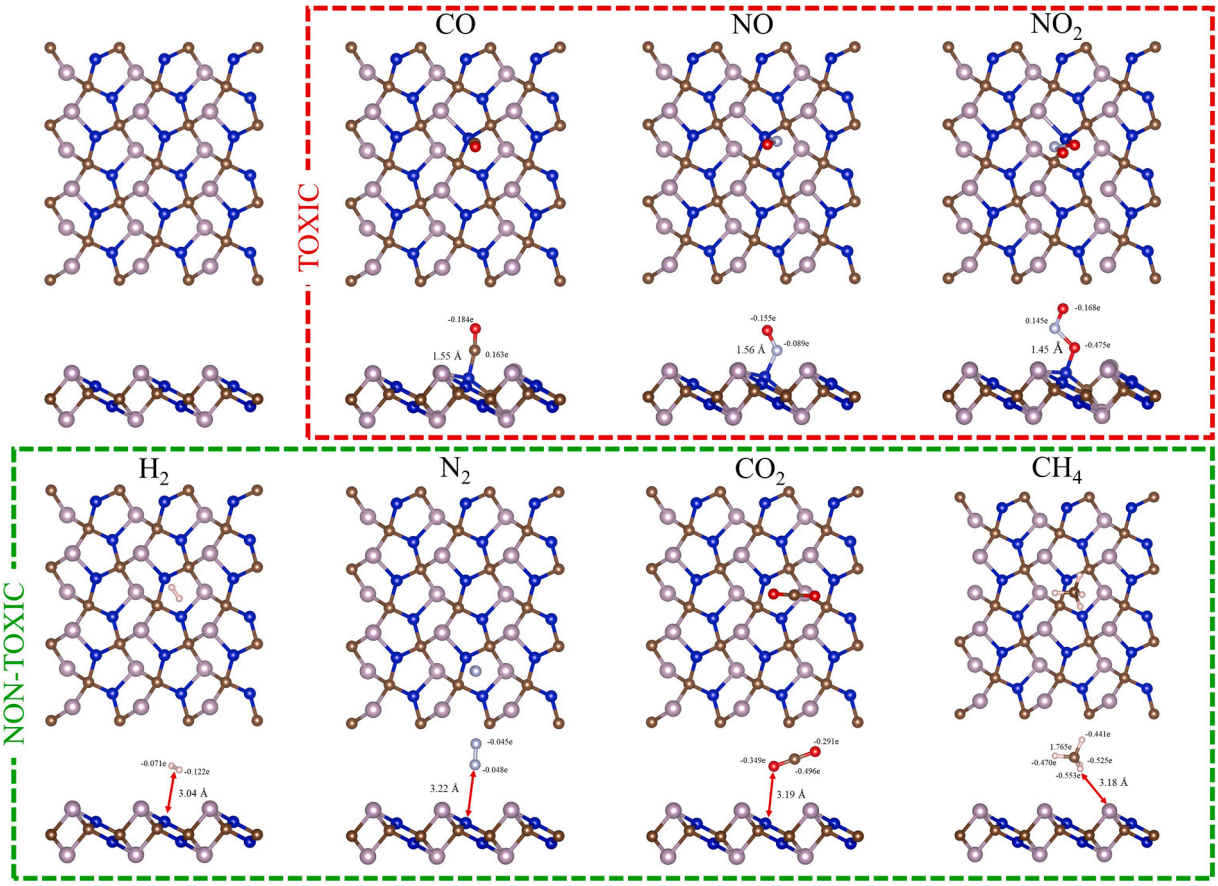

Fig. 2. 3 × 3 Supercell of pentagonal BCP geometrical structures with and without adsorbed toxic and non-toxic gases.

Table 1
Adsorption energy (E_{ad}), adsorption distance(d), and charge transfer (Q) of H_2, N_2, CO, CO_2, CH_4, NO and NO_2 on monolayer penta-BCP.

Gas Molecule	E_{ad}	d(Å)	$Q(\|e\|)$
H_2	− 0.079	3.07	− 0.055
N_2	− 0.122	3.22	− 0.040
CO	− 0.988	1.55	− 0.249
CO_2	− 0.198	3.19	− 0.068
CH_4	− 0.141	3.18	− 0.100
NO	− 1.010	1.56	− 0.325
NO_2	− 1.496	1.46	− 0.709

interference from these common environmental components. However, compared to penta-BCN, whose adsorption energies for toxic gases range from −0.90 to −1.68 eV for toxic CO, NO and NO_2 and −0.16 eV for non-toxic CO_2 eV,[37] both penta-BCP and penta-BeP_2 show lower adsorption strengths for the toxic gases CO, NO, and NO_2. This indicates that while penta-BCP offers better adsorption selectivity than penta-BeP_2, its adsorption strength for toxic gases is not quite as high as that of penta-BCN.

To gain further insight into the interaction mechanism between the adsorbed gas molecules and the penta-BCP monolayer, the charge transfer (Q) values were analyzed using Bader charge analysis [38], as shown in Table 1. These values quantify the electron flow between the gas molecules and the substrate. A negative Q indicates that electrons are transferred from the gas molecules to the sheet [39]. As observed in Table 1, all Q values are negative, showing that electron transfer occurs from the gas molecules H_2, N_2, CO, CO_2, CH_4, NO, and NO_2 towards the penta-BCP, in alignment with the behavior reported for penta-BCN [37].

We can see that the charge transfers in Table 1 have all negative values. This shows that electrons transfer from gas molecules such as H_2, N_2, CO, CO_2, CH_4, NO, and NO_2 into the penta-BCP, which behaves consistently with the penta-BCN reported. Notably, toxic gas molecules such as CO, NO, and NO_2 exhibit much stronger charge interactions, with electron transfers of − 0.249, − 0.325, and − 0.709 electrons, respectively, from these molecules to the penta-BCP. In contrast, non-toxic gas molecules such as H_2, N_2, CO_2, and CH_4 exhibit significantly weaker electron transfers, typically below − 0.100 electrons.

Furthermore, we calculated the charge density difference ($\Delta\rho$), which is defined as:

$$\Delta\rho = \rho_{\mathrm{BCP+gas}} - \rho_{\mathrm{BCP}} - \rho_{gas}, \tag{2}$$

where $\rho_{\mathrm{BCP+gas}}$ represents the charge density of the gas-adsorbed penta-BCP monolayer system. Similarly, ρ_{BCP} and ρ_{gas} represent the charge densities of the penta-BCP monolayer sheet and the gas molecule, respectively.

Fig. 3 (a) and (b) visualize the charge density difference ($\Delta\rho$) for non-toxic N_2 and toxic CO molecules adsorbed on a penta-BCP monolayer, respectively. Visualizations for the remaining gas molecules (H_2, CO_2, CH_4, NO, and NO_2) are presented in the Supplementary Information (Fig. S1). The yellow isosurfaces represent regions where electron density accumulates, while blue isosurfaces depict areas where electron density is depleted. The charge accumulation is significantly greater for the toxic CO molecule compared to the non-toxic N_2, further supporting the trend observed in their respective adsorption energies. This pattern holds for the other gas molecules as well: toxic NO and NO_2 exhibit greater charge accumulation compared to non-toxic H_2, CO_2, and CH_4.

We examined how gas molecule adsorption alters the electronic structure of the penta-BCP sheet in detail. Fig. 4 and the supplementary information (Figure S2) present the total and projected density of states

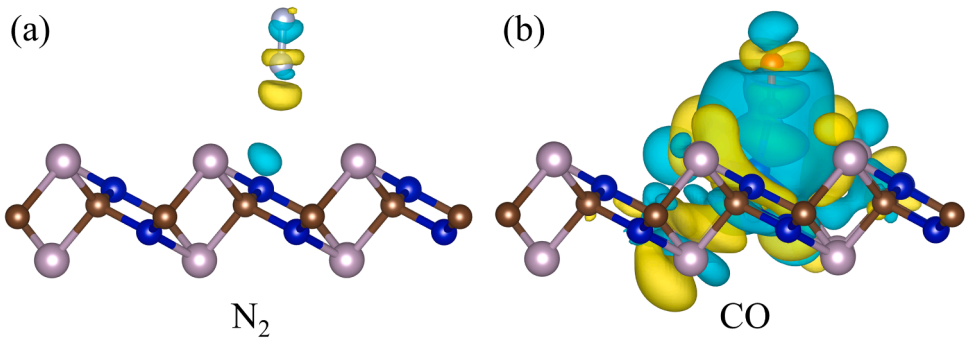

Fig. 3. Charge density difference for (a) N_2 and (b) CO gas molecules absorbed on penta-BCP. The isosurface is set to 0.003 e/Å^3.

(TDOS and PDOS) for the studied systems.

Notably, the strong interaction between the penta-BCP monolayer and the toxic gas molecules (CO, NO, and NO_2) significantly alters the DOS near the Fermi level (E_f), as shown in Fig. 4. A molecular peak emerges near the E_f for these toxic molecules (labeled in Fig. 4a, b, and c). Introducing new electronic states likely increases the carrier concentration within the penta-BCP monolayer. Conversely, the PDOS of non-toxic gas molecules (H_2, N_2, CO_2, and CH_4) shows minimal influence on the DOS of molecules near the Fermi level. Their molecular energy states lie far from the valence band maximum (VBM) and conduction band minimum (CBM). This observation suggests that the adsorption of non-toxic molecules has a negligible impact on the electronic structure of the penta-BCP monolayer. These adsorption-induced changes in the electronic structure are expected to affect the conductivity of the penta-BCP monolayer. This modulation of conductivity has the potential to serve as a response signal for detecting toxic gas molecules, as revealed in previous studies on MoS_2 [40], Ti_2CO_2 [41], and phosphorene [42].

To investigate how an electric field influences the sensing performance of the penta-BCP monolayer, we simulated the application of an external electric field along the Z- and $-Z$-directions by adding an artificial dipole sheet at the center of the simulation cell. Previous studies on penta-BCN have shown that the performance of 2D materials can be significantly altered by external electric fields [37]. Therefore, the adsorption characteristics of both toxic and non-toxic gases (H_2, N_2, CO, CO_2, CH_4, NO, and NO_2) under the influence of an external electric field applied perpendicular to the penta-BCP surface were examined. The electric field strength ranged from −0.5 V/Åto 0.5 V/Å, with the positive direction pointing upwards ($+Z$) and the negative direction downwards ($-Z$).

As shown in Fig. 5 and the Supplementary Information (Figure S3), the overall change in adsorption energy with electrical field resembles a parabola. Focusing specifically on the toxic gases CO, NO, and NO_2 (see Fig. 5), their adsorption energies became more negative as the electric field strength increased or decreased. This indicates that the applied electric field can effectively control the adsorption strength. These findings demonstrate that an applied electric field can manipulate the adsorption strength of gas molecules on the penta-BCP monolayer. By carefully controlling the electric field intensity, desirable adsorption characteristics tailored for specific gas sensing applications can be achieved. Furthermore, the adsorption distances (d) between the gas molecules and the penta-BCP monolayer decrease upon electric field application from 1.55 to 1.57 Å for NO, 1.42 to 1.48 Å for NO_2, and 1.54 to 1.56 Å for CO. These observations highlight the significant impact of the external electric field on the adsorption of toxic gases. Interestingly, some intriguing differences in how the electric field affects NO adsorption compared to what is observed for the penta-BCN monolayer were observed [37]. While the adsorption energy of NO on penta-BCN increased with a negative electric field, it exhibited a non-monotonic trend. NO adsorption on penta-BCN demonstrated a clear dependence on the electric field direction.

The recovery time (τ), the time required for a gas molecule to be desorbed from the sensor device, can be estimated using the following equation:

$$\tau = \nu_0^{-1} e^{-E_{de}/k_B T}, \tag{3}$$

where ν_0 is attempted frequency, which is the vibration frequency of the target molecule being adsorbed on the sensor surface. It is usually set as 10^{13} Hz, according to previous reports [5,43–45]. T is the temperature, k_B is the Boltzmann constant, and E_{de} is the desorption energy, which equals the adsorption energy because desorption is the inverse of adsorption. The recovery time of a gas sensor indicates how fast it returns to its original state after detecting a gas, which is crucial for its reusability.

As shown in Fig. 6, due to adsorption energies of around −0.99 to −1.50 eV for all toxic gas molecules, the penta-BCP monolayer exhibits recovery times of 4.03×10^3, 24.3, and 1.95×10^7 s for CO, NO, and NO_2 adsorption, respectively, at room temperature. Furthermore, the recovery time rapidly decreases with increasing temperature. The desorption process can be completed within 150 milliseconds at 500 K. This suggests that toxic gas molecules can be readily desorbed from the penta-BCP monolayer through heating. In comparison, the recovery time for a toxic NO molecule on penta-BeP_2 is 662.39 s at room temperature. Penta-BCP is far superior to penta-BeP_2 in terms of NO detection. Compared to other two-dimensional materials, such as the graphene/h-BN heterostructure (6.27×10^3 s) [46], BC_3 (4.43×10^5 s) [47], SiC(8.54×10^{-3} s) [48], Ti-doped h-BN (3.641×10^{18} s) [49], and the borophene/MoS_2 heterostructure (4.92×10^{11} s) [50], the penta-BCP monolayer stands out as an ideal reversible sensor for NO detection at room temperature. Due to its strong adsorption energy for toxic NO_2 gas, the penta-BCP material has a high recovery time. This makes it suitable for disposable NO_2 sensors.

Additionally, compared to the closely relative, the ternary penta-BCN, the penta-BCP monolayer demonstrated significantly faster recovery times. With the same attempt frequency of 10^{13} Hz, the reported recovery times for penta-BCN were 1.3×10^4, 390, and 2.1×10^{17} s for CO, NO, and NO_2 gas adsorption, respectively [37]. This highlights the superior performance of penta-BCP as a gas sensor.

4. Conclusions

In summary, our study demonstrates that the penta-BCP monolayer is a promising sensor material for differentiating toxic gases (CO, NO, and NO_2) from non-toxic gases (H_2, N_2, CO_2, and CH_4). The penta-BCP monolayer strongly interacts with toxic gas molecules such as CO, NO, and NO_2 but exhibits negligible interaction with non-toxic gases including H_2, N_2, CO_2, and CH_4. When an electric field is applied perpendicular to penta-BCP, the absorption energies of both toxic and non-toxic gases increase (more negative values). Therefore, the absorption energies can be tuned by applying an electric field. Due to its

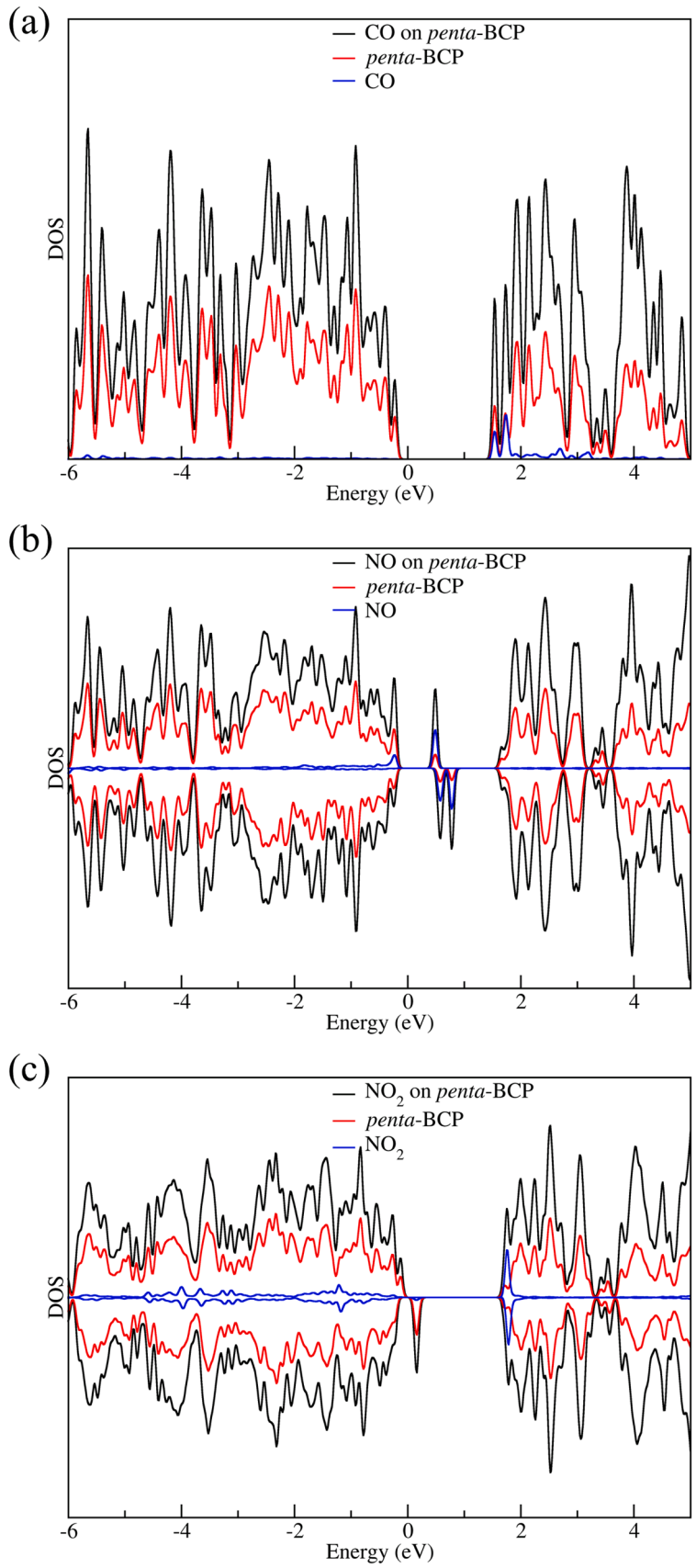

Fig. 4. Projected density of state (PDOS) for (a) CO, (b) NO, and (c) NO_2 molecules absorbed on penta-BCP. The Fermi level is set to zero.

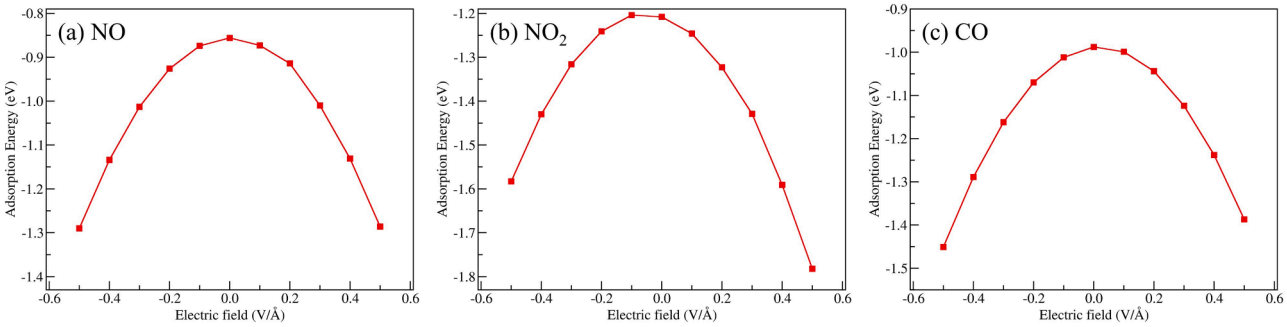

Fig. 5. Adsorption energies of toxic (a) NO, (b) NO_2, and (c) CO gas on penta-BCP surface as a function of applied electric field.

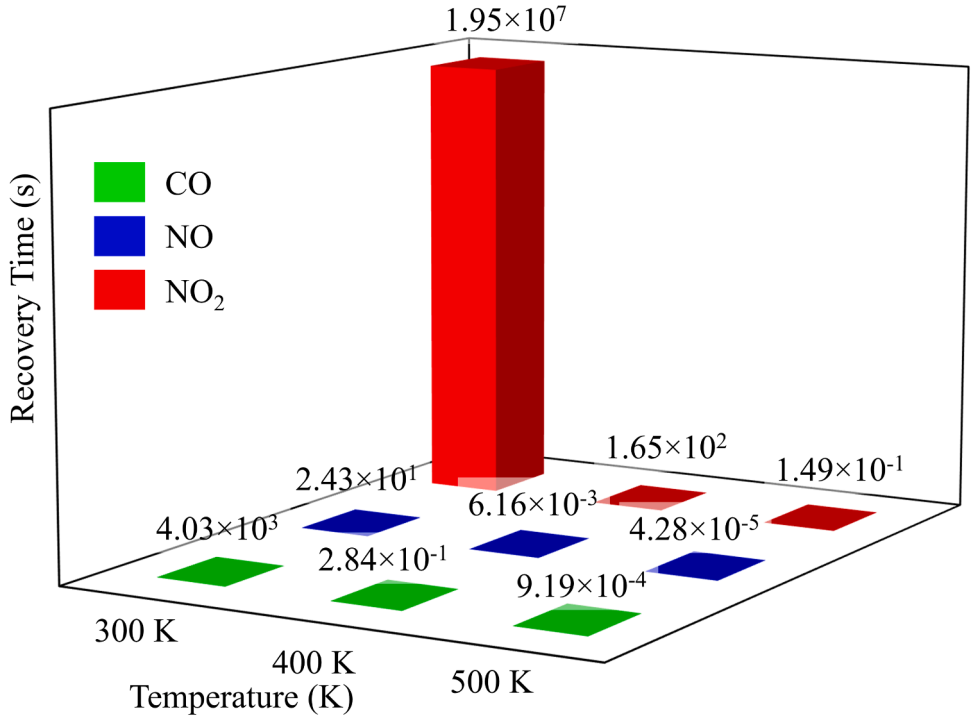

Fig. 6. Recovery times of toxic CO, NO, and NO_2 molecules at 300, 400, and 500 K.

strong adsorption of toxic gases,the penta-BCP monolayer also shows moderate recovery times. However, heating the sensor to 500 K effectively accelerates the desorption process, making it reusable. Among toxic gases, NO exhibits the shortest recovery time when adsorbed on penta-BCO, making it particularly suitable for NO gas detection. Moreover, compared to the closely relative, the ternary penta-BCN, the penta-BCP demonstrated superior performance as a sensor for toxic CO, NO, and NO_2 gases.

Associated content

Supporting Information

The charge density difference, the projected density of states, and the adsorption energy of non-toxic and toxic gas on penta-BCP monolayer as a function of an applied electric field are presented in the Supplementary Information, as mentioned in the text.

CRediT authorship contribution statement

Thanasee Thanasarnsurapong: Writing – original draft, Visualization, Validation, Methodology, Investigation, Formal analysis, Data curation, Conceptualization. **Suchanuch Sringamprom:** Writing – review & editing, Validation, Investigation, Data curation. **Pakpoom Reunchan:** Validation, Methodology, Supervision. **Weekit Sirisaksoontorn:** Writing – review & editing, Validation, Conceptualization. **Sirichok Jungthawan:** Validation, Methodology, Formal analysis. **Piyanooch Nedkun:** Writing – review & editing, Supervision, Methodology. **Jariyanee Prasongkit:** Writing – review & editing, Supervision, Formal analysis, Data curation. **Adisak Boonchun:** Writing – review & editing, Writing – original draft, Validation, Supervision, Software, Resources, Methodology, Formal analysis, Conceptualization.

Declaration of competing interest

The authors declare that they have no known competing financial interests or personal relationships that could have appeared to influence the work reported in this paper.

Acknowledgments

This project is funded by Kasetsart University Research and Development Institute, KURDI: YF(KU)52.66. T.T. is supported by the National Research Council of Thailand (NRCT), No. N41A661103. S.S. has

received funding support from Kasetsart University through the Graduate School Fellowship Program. A.B. has received funding support from the NSRF via the Program Management Unit for Human Resources & Institutional Development, Research and Innovation [grant number B39G670019]. Publication charges and proofreading were supported by International SciKU Branding (ISB), Faculty of Science, Kasetsart University. We wish to thank NSTDA Supercomputer Center (ThaiSC) for providing computing resources for this work.

Supplementary material

Supplementary material associated with this article can be found, in the online version, at 10.1016/j.talo.2025.100412

Data Availability

Data will be made available on request.

References

[1] F. Schedin, A.K. Geim, S.V. Morozov, E.W. Hill, P. Blake, M.I. Katsnelson, K. S. Novoselov, Detection of individual gas molecules adsorbed on graphene, Nat. Mater. 6 (9) (2007) 652–655.
[2] S. Mao, J. Chang, H. Pu, G. Lu, Q. He, H. Zhang, J. Chen, Two-dimensional nanomaterial-based field-effect transistors for chemical and biological sensing, Chem. Soc. Rev. 46 (22) (2017) 6872–6904.
[3] C. Anichini, W. Czepa, D. Pakulski, A. Aliprandi, A. Ciesielski, P. Samorì, Chemical sensing with 2D materials, Chem. Soc. Rev. 47 (13) (2018) 4860–4908.
[4] H.-S. Tsai, Y. Wang, C. Liu, T. Wang, M. Huo, The elemental 2D materials beyond graphene potentially used as hazardous gas sensors for environmental protection, J. Hazard. Mater. 423 (2022) 127148.
[5] T. Yang, X. Jiang, W. Yi, X. Cheng, T. Cheng, Enhanced fast response to Hg0 by adsorption-induced electronic structure evolution of Ti2C nanosheet, Appl. Surf. Sci. 544 (2021) 148925.
[6] X. Dong, T. Chen, G. Liu, L. Xie, G. Zhou, M. Long, Multifunctional 2D g-C4N3/MoS2 vdW heterostructure-based nanodevices: spin filtering and gas sensing properties, ACS Sens. 7 (11) (2022) 3450–3460.
[7] C. Luo, T. Chen, K. Cen, L. Xie, X. Dong, X. Xiao, Transition metal (Co, V, W, Zr) single-atom decorated biphenylene for enhancing the sensing performance of SF6 decomposition molecules, Langmuir 40 (18) (2024) 9490–9500.
[8] L. Xie, T. Chen, X. Dong, G. Liu, H. Li, N. Yang, D. Liu, X. Xiao, A comparative study of the electronic transport and gas-sensitive properties of graphene+, t-graphene, net-graphene, and biphenylene-based two-dimensional devices, ACS Sens. 8 (9) (2023) 3510–3519.
[9] S. Zhang, J. Zhou, Q. Wang, X. Chen, Y. Kawazoe, P. Jena, Penta-graphene: a new carbon allotrope, Proc. Natl. Acad. Sci. 112 (8) (2015) 2372–2377.
[10] M.-Q. Cheng, Q. Chen, K. Yang, W.-Q. Huang, W.-Y. Hu, G.-F. Huang, Penta-graphene as a potential gas sensor for NO x detection, Nanoscale Res. Lett. 14 (1) (2019) 306.
[11] C. Luo, N. Yang, X. Dong, D. Qin, G. Zhou, T. Chen, Susceptible detection of organic molecules based on C3B/graphene and C3N/graphene van der Waals heterojunction gas sensors, ACS Sens. 9 (9) (2024) 4822–4832.
[12] W. Yang, T. Chen, G. Zhou, Unveiling the tunable electronic, optoelectronic, and strain-sensitive gas sensing properties of janus ZrBrCl: Insights from DFT study, Appl. Surf. Sci. 680 (2025) 161283.
[13] J. Li, X. Fan, Y. Wei, G. Chen, Penta-BxNy sheet: a density functional theory study of two-dimensional material, Sci. Rep. 6 (1) (2016) 1–9.
[14] K. Zhao, Y. Guo, Y. Shen, Q. Wang, Y. Kawazoe, P. Jena, Penta-BCN: a new ternary pentagonal monolayer with intrinsic piezoelectricity, J. Phys. Chem. Lett. 11 (9) (2020) 3501–3506.
[15] K. Dabsamut, T. Thanasarnsurapong, T. Maluangnont, T. Jiraroj, S. Jungthawan, A. Boonchun, et al., Strain engineering and thermal conductivity of a penta-BCN monolayer: a computational study, J. Phys. D Appl. Phys. 54 (35) (2021) 355301.
[16] T. Thanasarnsurapong, K. Dabsamut, T. Maluangnont, S. Jungthawan, A. Boonchun, et al., Piezoelectric and electronic properties of hydrogenated penta-BCN: a computational study, J. Appl. Phys. 129 (9) (2021).
[17] K. Dabsamut, T. Thanasarnsurapong, I. Chatratin, T. Maluangnont, S. Jungthawan, A. Boonchun, Two-dimensional penta-niPS sheets: two stable polymorphs, J. Phys. Chem. C 126 (45) (2022) 19455–19461.
[18] K. Dabsamut, I. Chatratin, T. Thanasarnsurapong, T. Maluangnont, A. Boonchun, Theoretically proposed stable polymorph of two-dimensional pentagonal β-pdPSe, Phys. Chem. Chem. Phys. 25 (5) (2023) 3815–3819.
[19] C. Hou, Y. Shen, W. Sun, Y. Chen, D. Ni, Q. Wang, A penta-BCP sheet with strong piezoelectricity and a record high positive Poisson's ratio, J. Mater. Chem. C 10 (28) (2022) 10302–10309.
[20] K. Dabsamut, I. Chatratin, T. Thanasarnsurapong, S. Jungthawan, A. Boonchun, Surface alloy with sulfur leading piezoelectricity from non-piezoelectricity of pentagonal-pdPSe, J. Alloys Compd. 947 (2023) 169640.
[21] T. Thanasarnsurapong, P. Detrattanawichai, K. Dabsamut, I. Chatratin, T. Jiraroj, S. Jungthawan, A. Boonchun, et al., Ternary pentagonal BXN (X= C, Si, Ge, and Sn) sheets with high piezoelectricity, RSC Adv. 13 (14) (2023) 9636–9641.
[22] A. Ananchuensook, K. Dabsamut, T. Thanasarnsurapong, T. Maluangnont, T. Jiraroj, S. Jungthawan, A. Boonchun, et al., Towards a new packing pattern of li adsorption in two-dimensional pentagonal BCN, Phys. Chem. Chem. Phys. 24 (21) (2022) 13194–13200.
[23] T. Thanasarnsurapong, P. Detrattanawichai, K. Dabsamut, K. Simalaotao, T. Maluangnont, A. Boonchun, Enabling enhanced lithium storage capacity of two-dimensional pentagonal BN 2 by aluminum doping, J. Mater. Chem. C 11 (17) (2023) 5825–5830.
[24] N. Seniwong-Na-ayuttaya, T. Thanasarnsurapong, C. Wongchoosuk, K. Dabsamut, A. Boonchun, Exploring the impact of nonpatterned lithium packing on the high-capacity performance of penta-BSin, J. Phys. Chem. C (2025).
[25] X. Jiang, G. Zhang, W. Yi, T. Yang, X. Liu, Penta-BeP2 monolayer: a superior sensor for detecting toxic gases in the air with excellent sensitivity, selectivity, and reversibility, ACS Appl. Mater. Interfaces 14 (30) (2022) 35229–35236.
[26] S. Sringamprom, T. Thanasarnsurapong, T. Watcharatharapong, W. Hirunpinyopas, W. Sirisaksoontorn, J. Prasongkit, A. Boonchun, Monolayer Penta-BeAs2: a promising 2D materials for toxic gas sensor with high selectivity, ACS Appl. Mater. Interfaces 16 (41) (2024) 56387–56395.
[27] K. Lakhani, S. Kansara, S.K. Gupta, Y. Sonvane, D. Seifu, P.N. Gajjar, R. Ahuja, Dissociation of air pollutants on the uniform surface of pentagonal BeP2, Appl. Surf. Sci. 570 (2021) 151061.
[28] V.Q. Bui, T.-T. Pham, D.A. Le, C.M. Thi, H.M. Le, A first-principles investigation of various gas (CO, H2O, NO, and O2) absorptions on a WS2 monolayer: stability and electronic properties, J. Phys. Condens. Matter 27 (30) (2015) 305005.
[29] R.N. Somaiya, Y. Sonvane, S.K. Gupta, Adsorption of toxic gas molecules on the pre-oxidized Cu2Si nanosheet–a DFT study, Comput. Mater. Sci. 173 (2020) 109414.
[30] T. Hussain, D. Singh, S.K. Gupta, A. Karton, Y. Sonvane, R. Ahuja, Efficient and selective sensing of nitrogen-containing gases by si2BN nanosheets under pristine and pre-oxidized conditions, Appl. Surf. Sci. 469 (2019) 775–780.
[31] G. Kresse, J. Furthmüller, Efficiency of ab-initio total energy calculations for metals and semiconductors using a plane-wave basis set, Comput. Mater. Sci. 6 (1) (1996) 15–50.
[32] G. Kresse, J. Furthmüller, Efficient iterative schemes for ab initio total-energy calculations using a plane-wave basis set, Phys. Rev. B 54 (16) (1996) 11169.
[33] P.E. Blöchl, Projector augmented-wave method, Phys. Rev. B 50 (24) (1994) 17953.
[34] J.P. Perdew, K. Burke, M. Ernzerhof, Generalized gradient approximation made simple, Phys. Rev. Lett. 77 (18) (1996) 3865.
[35] H.J. Monkhorst, J.D. Pack, Special points for Brillouin-zone integrations, Phys. Rev. B 13 (12) (1976) 5188.
[36] S. Grimme, J. Antony, S. Ehrlich, H. Krieg, A consistent and accurate ab initio parametrization of density functional dispersion correction (DFT-D) for the 94 elements H-Pu, J. Chem. Phys. 132 (15) (2010).
[37] M. Wei, X. Dou, L. Zhao, J. Du, G. Jiang, Monolayer penta-BCN: a promising candidate for harmful gases detection, Sens. Actuators A Phys. 334 (2022) 113326.
[38] R.F.W. Bader, A.I. Molecules, A Quantum Theory, Clarendon: Oxford, UK, 1990.
[39] G. Henkelman, A. Arnaldsson, H. Jónsson, A fast and robust algorithm for Bader decomposition of charge density, Comput. Mater. Sci. 36 (3) (2006) 354–360.
[40] A. Shokri, N. Salami, Gas sensor based on MoS2 monolayer, Sens. Actuators B Chem. 236 (2016) 378–385.
[41] X.-f. Yu, Y.-c. Li, J.-b. Cheng, Z.-b. Liu, Q.-z. Li, W.-z. Li, X. Yang, B. Xiao, Monolayer Ti2CO2: a promising candidate for NH3 sensor or capturer with high sensitivity and selectivity, ACS Appl. Mater. Interfaces 7 (24) (2015) 13707–13713.
[42] S. Cui, H. Pu, S.A. Wells, Z. Wen, S. Mao, J. Chang, M.C. Hersam, J. Chen, Ultrahigh sensitivity and layer-dependent sensing performance of phosphorene-based gas sensors, Nat. Commun. 6 (1) (2015) 8632.
[43] J. Zhang, G. Yang, D. Yuan, J. Tian, D. Ma, A first-principles study of doped black phosphorus carbide monolayers as NO2 and NH3 sensors, J. Appl. Phys. 125 (7) (2019).
[44] K. Rajput, V. Kumar, D.R. Roy, Heterobilayer CaS/CaSe: a promising sensor for environmental toxic NO2 gas with high selectivity and sensitivity, Appl. Surf. Sci. 528 (2020) 146996.
[45] Z.-H. Yang, J.-H. Ren, T. Huang, W.-Q. Huang, W.-Y. Hu, G.-F. Huang, Two-dimensional chromium phosphorus monolayer based gas sensors to detect NOx: a first-principles study, Results Phys. 32 (2022) 105100.
[46] N.H. Raad, N. Manavizadeh, I. Frank, E. Nadimi, Gas sensing properties of a two-dimensional graphene/h-BN multi-heterostructure toward H2O, NH3 and NO2: a first principles study, Appl. Surf. Sci. 565 (2021) 150454.
[47] S.M. Aghaei, M.M. Monshi, I. Torres, S. Zeidi, I. Calizo, DFT study of adsorption behavior of NO, CO, NO2, and NH3 molecules on graphene-like BC3: a search for highly sensitive molecular sensor, Appl. Surf. Sci. 427 (2018) 326–333.
[48] Z. Zhao, Y. Yong, Q. Zhou, Y. Kuang, X. Li, Gas-sensing properties of the sic monolayer and bilayer: a density functional theory study, ACS Omega 5 (21) (2020) 12364–12373.
[49] B.A. Kalwar, W. Fangzong, A.M. Soomro, M.R. Naich, M.H. Saeed, I. Ahmed, Highly sensitive work function type room temperature gas sensor based on Ti doped hBN monolayer for sensing CO 2, CO, H 2 S, HF and NO. a DFT study, RSC Adv. 12 (53) (2022) 34185–34199.
[50] J. Shen, Z. Yang, Y. Wang, L.-C. Xu, R. Liu, X. Liu, The gas sensing performance of borophene/MoS2 heterostructure, Appl. Surf. Sci. 504 (2020) 144412.